OFDR Distributed Strain Measurements for SHM of Hydrostatic Stressed Structures: An Application to High Pressure Hydrogen Storage Type IV Composite Vessels - H2E Project

Laurent Maurin, Pierre Ferdinand, Fabien Nony, Stéphane Villalonga

7th European Workshop on Structural Health Monitoring
July 8-11, 2014. La Cité, Nantes, France

OFDR DISTRIBUTED STRAIN MEASUREMENTS FOR SHM OF HYDROSTATIC STRESSED STRUCTURES: AN APPLICATION TO HIGH PRESSURE H_2 STORAGE TYPE IV COMPOSITE VESSELS – H2E PROJECT

Laurent Maurin[1], Pierre Ferdinand[1], Fabien Nony[2], Stéphane Villalonga[2]

[1] *CEA, LIST, Optical Measurement Laboratory, F-91191 Gif-sur-Yvette, France.*
[2] *CEA, DAM, Polymer Synthesis and Processing Laboratory, F-37260 Monts, France.*

laurent.maurin@cea.fr

ABSTRACT

This paper deals with SHM of Composite Overwrapped Pressure Vessels (COPV) for high pressure hydrogen storage, based on embedded optical fibres and Rayleigh OFDR. Fibre Bragg Gratings *in situ* strain measurements on flat samples are first presented to assess the mechanical state of such anisotropic structures, and define a preliminary SHM criterion. Comparative fatigue tests were also performed on NOL rings to evaluate optical fibres mechanical impact, but their analysis in terms of energy revealed the difficulty to provide reliable results if the first cycles energy is not accurately controlled. Therefore, with no detrimental effect of the optical fibre embedment within the composite architecture, several instrumented pressure vessels were manufactured and tested. Accordingly, a mechanical criterion based on OFDR differential strain profiles analysis was defined to bring out internal defects, demonstrating the ability to early detect and locate internal flaws without requirements to inflate vessels at high pressures. Additionally, their sensitivity *vs.* pressure, analysed during a first burst test, provided additional valuable data about structure integrity. Finally, we define four complementary criteria based on *in situ* strain measurements to control pressure vessels for damage assessment, or any hydrostatic stressed structure since the underlying principles rely on strains proportionality *vs.* uniformly applied stresses.

KEYWORDS: *pressure vessel, optical fibre, Rayleigh OFDR, damage assessment.*

INTRODUCTION

Traditionally, metallic vessels have to comply with specific regulation rules (Pressure Equipment Directive from the European Parliament [1]) involving periodic requalifications. However, for high pressure composite vessels, standards, and particularly non-destructive techniques, have to be developed, tested and validated.

In this new frame, the French H2E research project aims at funding developments to set-up new control / monitoring techniques applicable to composite vessels, for both future regulatory and inspection needs. To reach the market, these techniques have also to be cost-effective in comparison with traditional ones.

To monitor such vessels and highlight the presence of structural defects, the CEA (LIST Institute and DAM) has conducted R&D based on high resolution distributed strain profiles analysis along singlemode optical fibres embedded into the composite structure.

To elaborate this method, preliminary tests were first carried out on samples to evaluate any significant intrusive effect of the optical fibres on their ultimate tensile strength and fatigue performance.

Then, several composite vessels were fully instrumented with optical fibres and tested up to their working pressure to validate the relevance of *in situ* distributed strain measurements to detect internal flaws thanks to a new and distributed differential strain criterion.

This criterion was validated during a first burst test, and then generalised to potentially lead, in the future, to "real-time" inspection of pressure storage vessels during isothermal filling operations.

This paper presents the results of this work carried out during the H2E project timeframe. It opens the way to future developments to extend this methodology to high pressure storage vessels controls during non-isothermal operations such as regular/fast gas-filling.

1 FIRST MECHANICAL TESTS ON FLAT SAMPLES – TOWARDS A FIRST CRITERION BASED ON *IN SITU* STRAIN MEASUREMENTS

1.1 First uniaxial tensile tests and optical fibre influence

Preliminary uniaxial tensile tests were first carried out on composite flat samples made of ten unidirectional plies to check for any significant mechanical influence of embedded optical fibres [2], considering that their quantity is several orders of magnitude greater than planned in pressure vessels.

Three different types of optical fibres were tested, differing by their coating in terms of outer diameter and composition. Results show that the average ultimate tensile strength of the control population still remains the greatest, but standard deviations for each batch are also too important to conclude to a significant optical fibres influence on the samples mechanical properties (Figure 1).

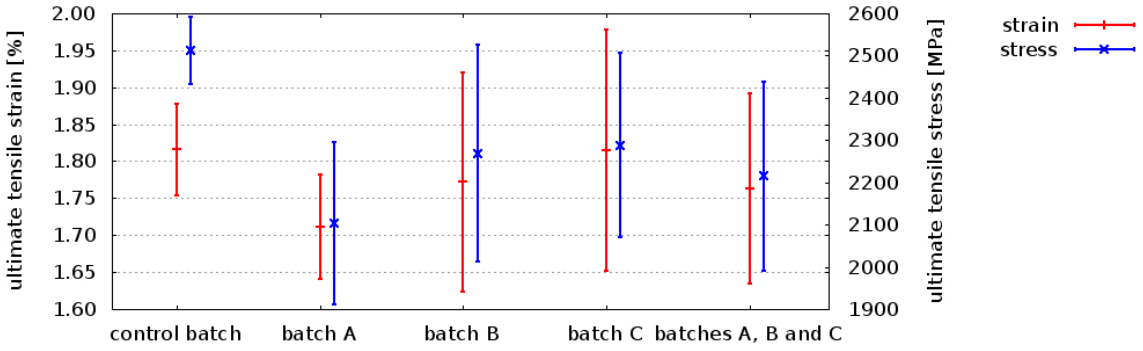

Figure 1: Uniaxial tensile tests conducted on unidirectional UD 0° flat samples [6]

1.2 *In situ* FBG strain measurements during tensile tests – A first damage criterion

Therefore, several composite flat specimens made of different ply orientations, more representative of a pressure vessel structure, were instrumented with Fibre Bragg Grating (FBG) transducers to monitor their internal strain during uniaxial tensile tests according to $\Delta\lambda_{Bragg}/\lambda_{Bragg} = 0.78 \times \Delta\varepsilon$ [3]. The FBG relative orientation *vs.* tensile effort direction depends on the instrumented plies, and takes values amongst 0°, 10°, 30°, 45°, 70°, 85° and 90°.

Then, FBG-based *in situ* strain measurements are compared with strains given by an electrical strain gauge mounted on surface. Tensile force is also recorded, which gives a good estimation of the sample average strain since carbon reinforcement fibres are purely elastic.

The experimental results clearly show that matrix debonding appears once *in situ* FBG strain measurements differ significantly from surface and average strains measurements, and this phenomenon appears even earlier if the difference between the tensile effort direction and the instrumented ply orientation is increased (Figure 2).

These observations suggest the elaboration of a first criterion to detect composite structure damages based on the difference between the average strain (standing for the whole structure) and the *in situ* local strain where damages occur.

Thus, the underlying idea for pressure vessel inspection will be to extend this restricted area criterion, given by a single FBG transducer, to distributed measurements all over the pressure vessel thanks to the Rayleigh OFDR technique (§ 3).

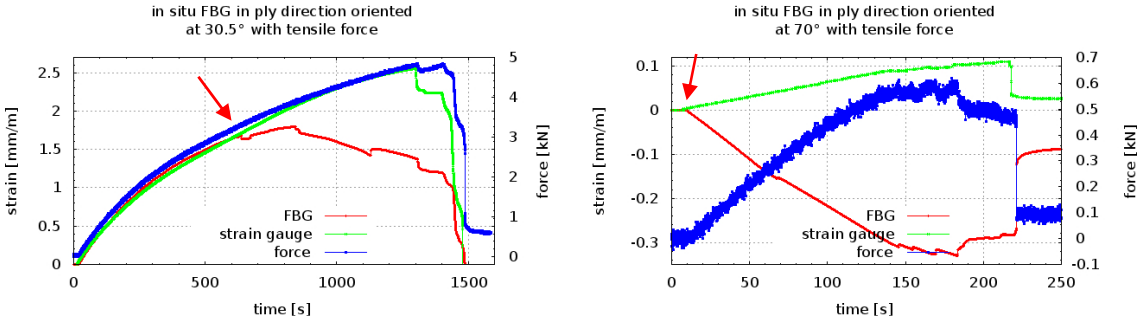

Figure 2: *In situ* (FBG) compared with surface (strain gauge) measurements during uniaxial tensile tests [6]

2 LOW-CYCLE FATIGUE TESTS, AND ENERGY CONSIDERATIONS

Meanwhile, comparative fatigue tests on NOL rings [4], more representative of pressure vessels, were performed to evaluate the optical fibres mechanical impact on the cylindrical shell. As usual, several ply orientations representing four different composite structures were considered (Figure 3).

Figure 3: Experimental set-up (left) and NOL ring after failure (right)

The low-cycle frequency was equal to 0.4 Hz and the maximum displacement Δh was tuned to reach failure after 15,000 cycles for each batch. Force F and position h were continuously recorded to compute an energy parameter E_{cycle} according to Equation (1). This parameter also reflects the dissipated strain energy during each cycle.

$$E_{cycle} = \left|E_{half-cycle_{up}}\right| + \left|E_{half-cycle_{down}}\right| \quad \text{with:} \quad E_{h_0 \to h_0+\Delta h} = \int_{h_0}^{h_0+\Delta h} F(u)\, du \qquad (1)$$

This parameter is more relevant in comparison with a traditional force *vs.* time analysis, since samples strength interpreted in energy always decreases, expressing a progressive damage, especially during the few first cycles, whereas interpreted in force amplitude, it is not systematically true. This difference also probably reflects reorientations of reinforcement carbon fibres under stress (Figure 4).

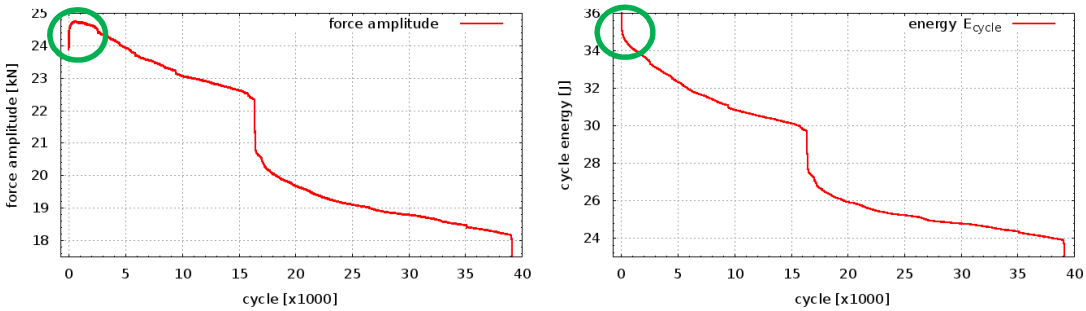

Figure 4: Typical low-cycle fatigue test expressed in force amplitude (left) and in energy (right) [6]

Experimental data gathered during fatigue tests lead to a correlation between the first thousands cycles strain energy average sensitivity $\langle S_E \rangle$ and the first cycles average strain energy $\langle E_{N=0} \rangle$. Therefore, these first cycles are crucial for the subsequent damage rates (Figure 5).

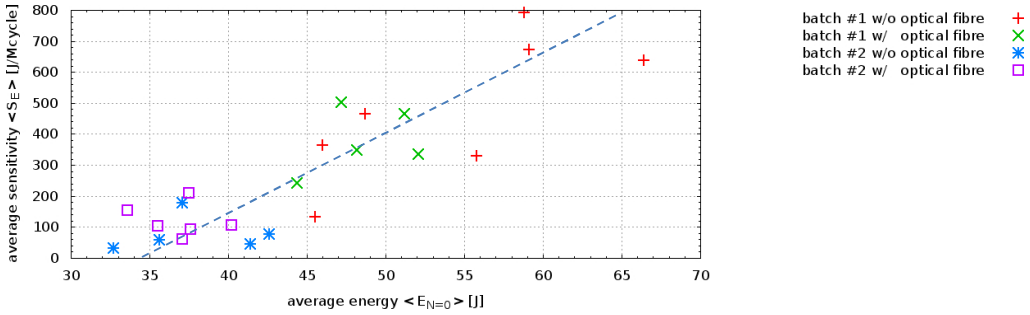

Figure 5: Strain energy average sensitivity $\langle S_E \rangle$ *vs.* first cycles average strain energy $\langle E_{N=0} \rangle$ [6]

The relative contribution on the number of cycles to failure δN of this starting energy can therefore be estimated according to Equation (2), taking into account:

- the strain energy average sensitivity $\langle \boldsymbol{S_E} \rangle$ during the first thousands cycles,
- the average starting energy $\langle \boldsymbol{E_{N=0}} \rangle$ for each batch,
- the displacement $\boldsymbol{\Delta h}$ for each cycle,
- the position reproducibility $\boldsymbol{\delta h}$ on the testing machine,
- the strain energy dispersion $\boldsymbol{\Delta E_{N=0}}$ at start for a same batch.

$$\delta N_{\delta h} \approx \frac{1}{\langle S_E \rangle} \frac{\langle E_{N=0} \rangle}{\Delta h} \delta h \quad \text{and} \quad \delta N_{\Delta E_{N=0}} \approx \frac{\Delta E_{N=0}}{\langle S_E \rangle} \tag{2}$$

This analysis highlights the major influence of the strain energy dispersion $\Delta E_{N=0}$ during the first fatigue cycles, considering a typical error for δh better than 2 μm on the test machine. Monitoring these tests in terms of energy would have been a better solution to reduce their dispersion. Concluding about any optical fibre influence on cycles to failure would then have been irrelevant (Table 1).

Table 1: Position reproducibility $\delta N_{\delta h}$ and starting energy dispersion $\delta N_{\Delta E_{N=0}}$ impacts on cycles to failure

batch	$\langle \boldsymbol{S_E} \rangle$ [J/Mcycle]	$\langle \boldsymbol{E_{N=0}} \rangle$ [J]	$\boldsymbol{\Delta E_{N=0}}$ [J]	$\boldsymbol{\Delta h}$ [mm]	$\boldsymbol{\delta N_{\delta h}}$ [cycle/µm]	$\boldsymbol{\delta N_{\Delta E_{N=0}}}$ [cycle/J]
#1 w/o optical fibre	484.64	45	20.9	1.92	**48.36**	**2063**
#1 w/ optical fibre	378.58	40	9.5	1.92	**55.03**	**2641**
#2 w/o optical fibre	77.71	34	9.9	1.65	**265.16**	**12868**
#2 w/ optical fibre	121.2	34	6.6	1.65	**170.02**	**8251**

However, *post mortem* analyses show, as expected [2], the perfect integration of optical fibres in the composite matrix since no void nor delamination appear in their vicinity (Figure 6).

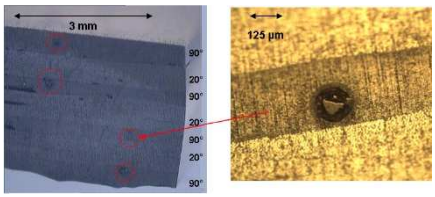

Figure 6: NOL ring *post mortem* analysis under microscope after low-cycle fatigue test [6]

3 STRUCTURAL DEFECT DETECTION AND DIFFERENTIAL DISTRIBUTED STRAIN ANALYSIS

On this basis, several composite pressure vessels were fully instrumented with optical fibres at different depths inside the matrix, from sub-surface to liner vicinity. Some of these structures were deliberately damaged, then inflated with water to avoid crosstalk temperature effects.

The distributed State Of Polarisation (SOP) for each optical fibre is then recorded thanks to Rayleigh-based Optical Frequency Domain Reflectometry (OFDR) with a Luna™ OBR-4600 instrument, and post-processed to compute strain profiles $\Delta\varepsilon(s)$ along the curvilinear position s in the composite structure [5].

The criterion first defined on flat samples (§ 1.2) is then extended according to the following assumptions, assuming that defects may be scattered anywhere into the structure [6]:

- *an hypothesis is to consider internal defects as structural weaknesses resulting, in their vicinity, in local strains different from the rest of the structure supposed undamaged,*
- *by a set of differences between strain measurements, it must be possible to bring them out.*

This mechanical criterion $\boldsymbol{\delta_K \Delta\varepsilon}$ can be expressed according to Equation (3) taking into account [7]:

- a first strain variation $\Delta\boldsymbol{\varepsilon_{P_0 \to P_{ref}}}$ between inflation pressures P_0 and P_{ref},
- a second strain variation $\Delta\boldsymbol{\varepsilon_{P_0 \to P}}$ between inflation pressures P_0 and P,
- a proportionality coefficient $\boldsymbol{K_{(P_0, P_{ref}, P)}}$ calculated by least-squares minimisation of $\|\delta_K \Delta\varepsilon\|$.

$$\delta_K \Delta\varepsilon_{(P_0, P_{ref}, P)}(s) = \Delta\varepsilon_{P_0 \to P}(s) - K_{(P_0, P_{ref}, P)} \times \Delta\varepsilon_{P_0 \to P_{ref}}(s) \tag{3}$$

The $\delta_K \Delta\varepsilon$ criterion is in fact an error function whose significant deviations from zero point out local abnormal mechanical behaviours, in other words: structural defects.

Pressure P_0 can be any value; however, for the sake of simplicity, it usually corresponds to an empty pressure vessel. In this frame, several structures were tested, up to $700\ bar$ working pressure. Control pressures P_{ref} and P, for these experiments, were much smaller than working pressure, typically $P_{ref} = 100\ bar$ and $P = 150\ bar$ (Figure 7).

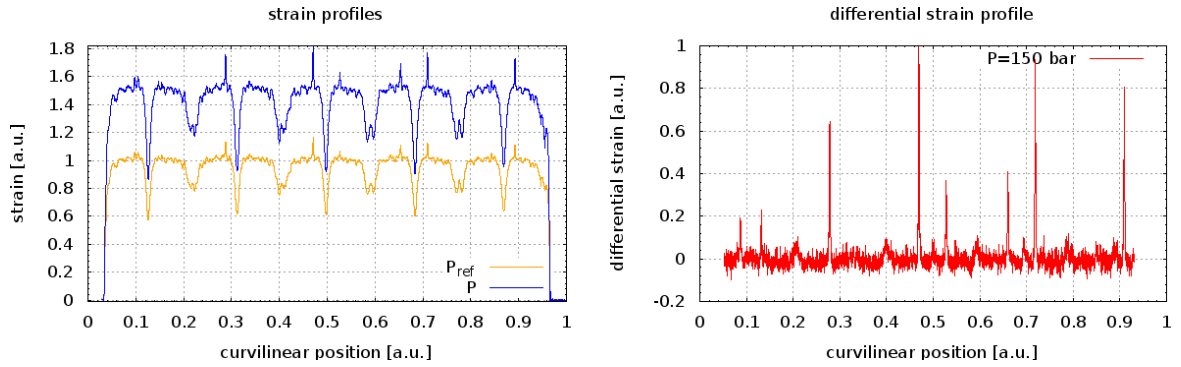

Figure 7: Differential strain profile $\delta_K \Delta\varepsilon(s)$ – $P_{ref} = 100\ bar$ and $P = 150\ bar$ ($P_0 = P_{atm}$) [6]

Furthermore, OFDR signal-to-noise ratio and centimetre spatial resolution are good enough to enable inspections at even lower pressures, *e.g.:* $P_{ref} = 100\ bar$ and $P = 40\ bar$. It is then possible to start to control pressure vessels at minimum pressure as low as 6% of service pressure without any risk for additional damages induced by the inspection protocol (Figure 8, *left*).

But in some cases, due to strain redistributions under stress, some defects may change to behave like the rest of the structure, disappearing from subsequent analyses. Nevertheless, it is sometimes possible to select more appropriate control pressures to bring out their residual strains once the pressure vessel is deflated (Figure 8, *right*).

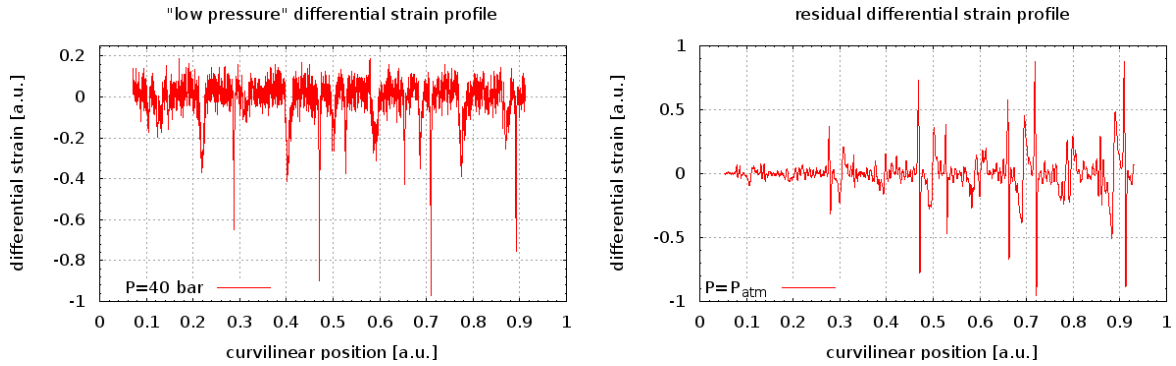

Figure 8: Differential strains with $P = 40\ bar$ (left) and residual differential strains with $P = P_{atm}$ (right)

4 FIRST BURST TEST AND COMPLEMENTARY ANALYSES

Since the $\delta_K \Delta\varepsilon$ parameter has proven to be efficient even below service pressure, it has also been tested at higher pressures, at least one magnitude order greater than previous control pressures, during a first burst test (Figure 9).

Figure 9: Composites Aquitaine™ pressure vessel burst test facility

The reservoir is filled with room-temperature water to avoid crosstalk effects on measurements, pressure steps are typically equal to some tens of bar. In this configuration, it is possible to both [7]:

- ensure strain measurements $\Delta\boldsymbol{\varepsilon}_{\boldsymbol{P_{i-1}\rightarrow P_i}}$ between pressure steps without post-processing error,
- compute, without additional artefact, strain variations $\Delta\boldsymbol{\varepsilon}_{\boldsymbol{P_0\rightarrow P_n}}$ for any pressure step P_n according to Equation (4) (Figure 10).

$$\Delta\varepsilon_{P_0\rightarrow P_n}(s) = \sum_{i=1}^{i=n} \Delta\varepsilon_{P_{i-1}\rightarrow P_i}(s) \tag{4}$$

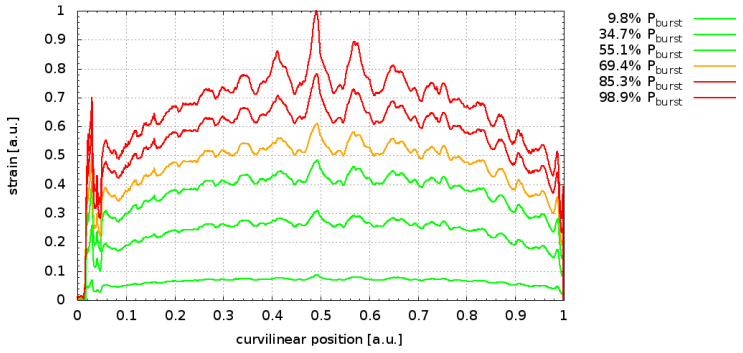

Figure 10: Strain profiles $\Delta\varepsilon_{P_0\rightarrow P_n}(s)$ during water-filling operation: baseline for structural monitoring regarding theoretical mechanical properties of the composite structure

It is also possible to benefit from the pressure steps data to differentiate the differential strain profile $\delta_K \Delta\varepsilon(s)$ *vs.* pressure, to evaluate a sensitivity $\mathcal{S}_{(P_0,P_{ref},P)}(s)$ according to Equation (5).

$$\mathcal{S}_{(P_0,P_{ref},P)}(s) = \frac{\partial \delta_K \Delta\varepsilon_{(P_0,P_{ref},P)}(s)}{\partial P} \Rightarrow \mathcal{S}_{(P_0,P_{ref},P)}(s) \approx \frac{\delta_K \Delta\varepsilon_{(P_0,P_{ref},P+\Delta P)}(s) - \delta_K \Delta\varepsilon_{(P_0,P_{ref},P)}(s)}{\Delta P} \quad (5)$$

This parameter gives additional information about structural defects evolution during reservoir filling, and should also be helpful to early detect and locate, *e.g.*: a crack propagation (Figure 11).

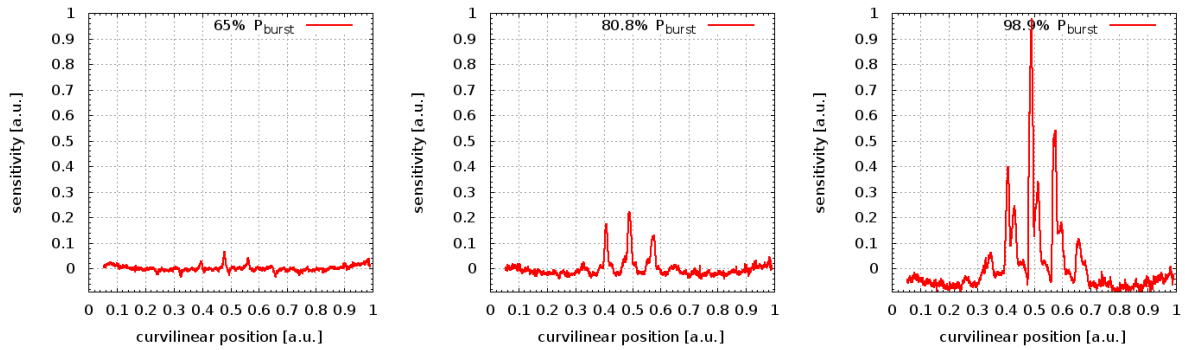

Figure 11: Differential strain sensitivity *vs.* pressure profile $\mathcal{S}_{(P_0,P_{ref},P)}(s)$: "instantaneous" strain deviations due to structural defects highlighted during the filling operation

Finally, since carbon reinforcement fibres are elastic, there should be a relationship $\mathcal{D}$ between the proportionality coefficient K and the inflation pressure P. Then, assuming that without any defect, $K = K_0$, such a relationship could be expressed according to Equation (6).

$$\mathcal{D}_{(P_0,P_{ref})}(P) = \frac{P\left(K_{0(P_0,P_{ref},P)}\right) - P\left(K_{(P_0,P_{ref},P)}\right)}{P_{burst}} \quad (6)$$

This damage assessment parameter $\mathcal{D}$ clearly revealed, during the burst test, a critical and global damage roughly starting at 70% burst pressure, and demonstrated its robustness to give relevant results even with sparse data, for instance, in case of optical fibre break (Figure 12, *left*).

It took a maximum value equal to 2.49% at 98.9% burst pressure during this first experiment (Figure 12, *right*). Also, this may be the signature of a crack propagation.

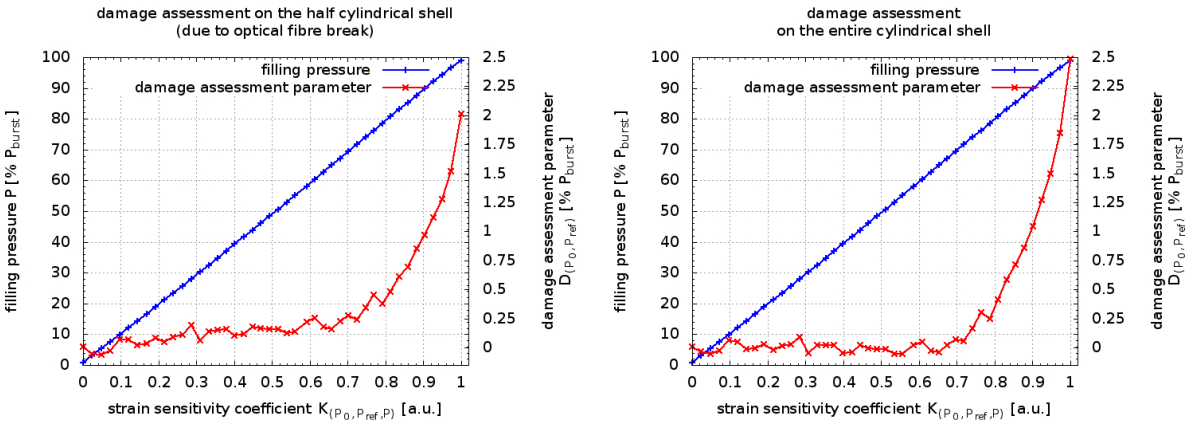

Figure 12: Pressure vessel damage assessment: evidences of critical damage starting at 70% burst pressure

CONCLUSION

Based on the fact that composite pressure vessels are subjected to an homogeneous hydrostatic stress (the filling pressure), we demonstrated, according to OFDR measurements on composite vessels interpreted in terms of differential strains, the ability to detect some structural defects without the need to inflate them at high pressures (from few MPa up to working pressure), thus reducing global cost of operation and risks of creation, or evolution, of new or existing defects.

Four complementary criteria based on distributed strain and pressure vessel measurements during the water-filling operation are proposed for pressure vessels monitoring and control. Provided that real-time OFDR measurements will be achievable in a near future, we could therefore rely on an efficient and easily understandable SHM procedure for such structures, but also for any structure submitted to hydrostatic stress.

Besides the fact that these optical measurements provide information of a mechanical nature (*i.e.*: the distributed strain profile all along the optical fibre), they are performed by the same distributed sensor (the optical fibre itself) embedded into the composite structure throughout its lifetime, eliminating by design any measurement dispersion due to replacement, *e.g.* for maintenance purposes.

Thus, the optical fibre used in combination with Rayleigh OFDR appears to be a relevant high-end and *in situ* non-destructive measurement technique for long-term SHM of high pressure vessels.

ACKNOWLEDGEMENTS

Authors thank their H2E partners, Composites Aquitaine™ and Air Liquide™, for their technical support and availability, and OSEO for co-funding this project.

REFERENCES

[1] European Parliament. *Directive 97/23/EC of the European Parliament and the Council of 29 May 1997 and the approximation of the laws of the Member States concerning pressure equipment*. *OJ L 181* (1997).

[2] Sansonetti, P. *et al.* Intelligent composites containing measuring fiber-optic networks for continuous self-diagnosis. 198–209 (1991). doi:10.1117/12.50179

[3] Ferdinand, P. Capteurs à fibres optiques à réseaux de Bragg. in *Techniques de l'ingénieur, R 6735* 1–24 (1999).

[4] ASTM Standard D2290 - 08 Standard Test Method for Apparent Hoop Tensile Strength of Plastic or Reinforced Plastic Pipe by Split Disk Method. (2008). doi:10.1520/D2290-08

[5] Froggatt, M. & Moore, J. High-Spatial-Resolution Distributed Strain Measurement in Optical Fiber with Rayleigh Scatter. *Appl. Opt.* **37**, 1735–1740 (1998).

[6] Maurin, L. *et al.* Contrôle santé par fibres optiques de réservoirs composites pour le stockage d'hydrogène sous haute pression - Projet H2E (Horizon Hydrogène Énergie). in *Instrumentation & Interdisciplinarité – Capteurs Chimiques & Physiques* 39–44 (EDP Sciences, 2013).

[7] Maurin, L. Librairie de calcul de profils différentiels d'écarts de déformations longitudinales le long d'une abscisse curviligne (recherche de défauts de structure). (CEA, 2013). IDDN.FR.001.530003.000.S.P.2013.000.30000